

inter noise

2013 | INNSBRUCK | AUSTRIA



15.-18. SEPTEMBER 2013

NOISE CONTROL FOR QUALITY OF LIFE

A comparison between Finite Element and Waveguide Finite Element Methods for the simulation of tire/road interaction

Carsten Hoever¹, Achillefs Tsotras², Ernst-Ulrich Saemann³, and Wolfgang Kropp⁴

^{1,4} Division of Applied Acoustics, Chalmers University of Technology, SE-41296 Gothenburg, Sweden

^{2,3} Continental Reifen Deutschland GmbH, Jaedekamp 30, 30419 Hannover, Germany

ABSTRACT

Due to increasing road utilization and tightening regulations, an increasing effort is made by the tire and automotive industries for accurate modeling of tire/road noise. It is well known that finite element (FE) based methods describing the vibration response of a rolling tire are computationally expensive while analytical models do not offer the necessary accuracy in the structural description of the tire. The recently proposed waveguide finite element (WFE) method combines the detailed description of a discretized tire cross section with a computationally efficient wave approach in the circumferential direction. The method has been successfully applied for tire dynamics and rolling noise simulations. An important aspect for the modeling of rolling noise is an accurate description of the road induced excitation. Both the high frequency vibration field and the lower frequency or quasi-static contact area need to be accurately captured. In this work we compare FE and WFE models of a tire in terms of traditional NVH properties such as mobility and modal frequencies, and in term of contact behavior such as footprint shape and structural stiffness. This way the potential of the WFE method for the modeling of both the excitation and the response of a rolling tire is critically examined.

Keywords: Tire Dynamics, Simulation, Numerical Methods

1 INTRODUCTION

In the last years the public awareness for the health benefits associated with a reduction of tire/road noise has increased. As there is sustained demand for personal mobility and transportation services in society, it seems unlikely that a decrease in noise levels be achieved by traffic reduction. Instead roads, vehicles, and tires have to be optimized with regards to noise generation. This has been acknowledged by policy makers, leading to a set of new, tightened regulations (e.g. [1, 2]). In view of this, an increasing effort is made by the tire and automotive industries for accurate modeling of tire/road noise.

A rolling tire is a complex dynamic system. Several physical mechanisms contribute to rolling noise. It is usually distinguished between vibrational and aerodynamical mechanisms, and propagation effects. Of these the vibrational mechanisms are the dominating source terms below 1 kHz to 1.6 kHz at the most

¹ carsten.hoever@chalmers.se

² achillefs.tsotras@conti.de

³ ernst-ulrich.saemann@conti.de

⁴ wolfgang.kropp@chalmers.se

common driving speeds of 30 km/h to 100 km/h [3]. The tire/road interaction leads to time-varying changes of the tire geometry which ultimately result in sound generation. The scope of the tire/road interaction ranges from large-scale, low-frequency running deflections of the tire tread, belt and sidewall at the leading and trailing edges of the contact zone to small-scale, high-frequency tire excitation by time varying contact forces due to tread patterns or road texture. Of additional importance is the so-called horn-effect, a propagation effect which significantly amplifies major parts of sound radiation [4]. The horn-effect is strongly dependent on the large-scale deformations of the tire in the footprint area. Summing up, a tire model suitable for rolling noise predictions needs to adequately capture both the high frequency vibration field and the low frequency deformations and quasi-static contact area.

Since the mid-1960s, a variety of different models for simulating the dynamic response of tires have been developed. These range from analytical models, based on more or less coarse simplifications of the geometrical and material properties, to highly sophisticated numerical models, accounting for the detailed physical properties of tires. One of the first models was presented by Böhm [5]. He calculated low frequency free and forced responses of a tire by modeling it as a pretensioned, circular ring on an elastic foundation. Through the years, many variations of the same basic approach have been used to model various aspects of tire dynamics, e.g. [6, 7, 8]. Ring models perform quite well for frequencies below roughly 300 Hz or 400 Hz but generally fail for higher frequencies at which wave propagation across the tire cross section starts. This is because the approach do not allow for lateral wave propagation.

Kropp [9] proposed a method to overcome this shortcoming by modeling the complete assembly of belt and sidewalls as an pretensioned, orthotropic plate on an elastic foundation. Agreement between modeled and measured input mobilities was good up to 2 kHz, with the exception of the lower frequency regions which were negatively affected by the negligence of curvature. Several variations Kropp's model have been presented in literature [10, 11]. Further analytical shell/plate models have been proposed by Pinnington [12] and Lecomte *et al.* [13]. All analytical models have in common that they are usually comparably simple and fast, and often provide worthwhile insight into physical processes. However, problems arise due to the geometrical simplifications inherent to all of the models.

The rapid development of computer capacity during recent decades has made it possible to perform detailed numerical modeling of tires using finite element methods (FEM). While early FE models (e.g. [6, 14]) were geometrically only slightly more complex than their analytical counterparts, current implementations are detailed enough to individually model nearly every different material group in the tire [15, 16]. FE based tire dynamics models have been the basis for a number of different applications [6, 15, 16, 17].

Generally, FE models have proven to be valuable tools. They are flexible and can easily account for non-linearities, complex materials and geometries. Using FE, objects and processes which are far too complicated to be covered by analytical models can be easily simulated. The use of commercial FEM software can reduce implementation time and the widespread use in industry facilitates data exchange. However, there are still two major problems associated with FEM. Firstly, finite element calculations often provide less insight into the physical processes leading to a result than a comparable analytic model (assuming that this exists). Secondly, requirements on computer capacity are high. The available computation power limits the discretization size which in turn determines the upper frequency limit of the simulations. Due to this, simulations are usually restricted to frequencies below approximately 1 kHz. Even with today's computational resources it seems hardly practical to use FEM for parameter studies covering the whole relevant frequency region for tire/road noise, i.e. up to around 2 kHz.

In order to reduce computational costs several approaches which combine parts of traditional FE modeling with analytical methods have been presented in recent years. One of these is the waveguide finite element method (WFEM) [18, 19]. In this technique the tire is considered to have constant cross sectional material and geometrical properties along the circumference. This allows to combine FE modeling of the cross-section with a wave propagation ansatz in the circumferential direction. The resulting eigenvalue problem is formulated in the wave domain and requires specially developed elements. Computational costs remain low because only the cross section of the tire is modeled numerically.

Waki *et al.* [20] presented a similar approach in which the tire is considered as a periodic structure

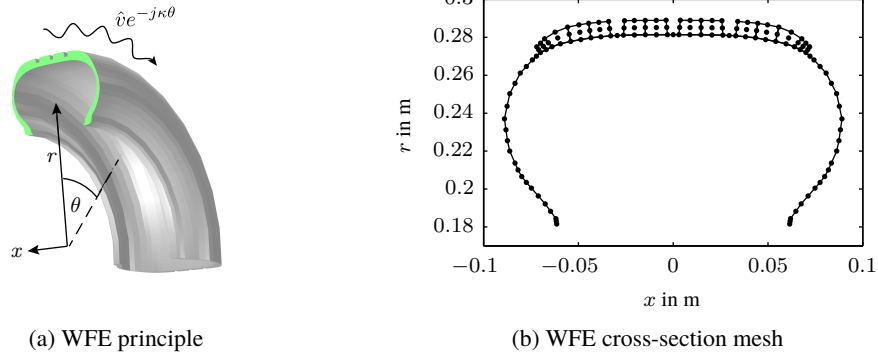


Figure 1 – (a) The tire as a curved waveguide: for the cross-section (marked in green) in the (x, r) -plane an FE approximation is used, while in circumferential direction θ wave propagation is assumed. Waves traveling in negative θ direction have to be considered as well, but are not shown here. (b) WFE mesh of the 175/65 R14 tire cross section. Nodes marked by ●.

along the circumference. Initially, a short section of the waveguide is modeled using standard commercial FEM. A periodicity condition is then applied. This results in an eigenvalue problem from which the forced response can be calculated using a wave approach. Numerical efficiency is again high and in contrast to the WFEM approach there is no need for specially designed elements. Alas, the method seems to be prone to numerical problems [21].

In this study a waveguide finite element tire model as described in [19, 22] is compared with a standard FE model of the same tire. Comparisons are made regarding both quasi-static properties such as footprint size and load-deflection behavior, and dynamic properties, i.e. free and forced response. The FE model has been developed with a focus on the good representation of the tire’s static contact area while the WFE model has been tuned to give good correlation to a mobility test. In that sense each of the two models can be considered as a static or dynamic simulation reference for their respective counterpart.

Sections 2 and 3 give an overview of the used FE and WFE tire models. In Section 4 the input data is described. The results of the quasi-static and dynamic simulations are presented in Section 5 and discussed in Section 6. The paper ends with some final remarks in Section 7.

2 THE FINITE ELEMENT TIRE MODEL

The finite element representation of the tire is based on a software developed and used by Continental AG. For the particular task a 3D model composed of 100 radial sections is used. The rubber components of the tire are modeled with brick elements using a hyperelastic material law. A composite formulation is used for the construction zones with cord reinforcement. The inflated-loaded tire equilibrium for the comparison of the contact deformation and the radial stiffness is calculated with a nonlinear algorithm which takes the pressure induced stress condition into account. The eigenanalysis is performed under consideration of the temperature and frequency dependency of the viscoelastic properties. Forced response is calculated using the derived modally decomposed model.

3 THE WAVEGUIDE FINITE ELEMENT TIRE MODEL

The used waveguide finite element approach is identical to the one described in [19, 23]. A waveguide is a system with constant geometrical and material properties along one (typically “long”) dimension. In this dimension, the motion can be described by a set of propagating waves fulfilling the boundary conditions imposed by the waveguide characteristics. In this sense, and with reference to Figure 1a, a tire is a waveguide for which the motion along the circumferential dimension can be described by waves fulfilling a periodicity condition $\mathbf{u}(\theta) = \mathbf{u}(\theta \pm 2\pi)$, where \mathbf{u} is the tire displacement and θ the circumferential angle. The waveguide property is used in conjunction with conventional two-dimensional finite element modeling of the waveguide cross-section, see Figure 1b. For a cylindrical coordinate system

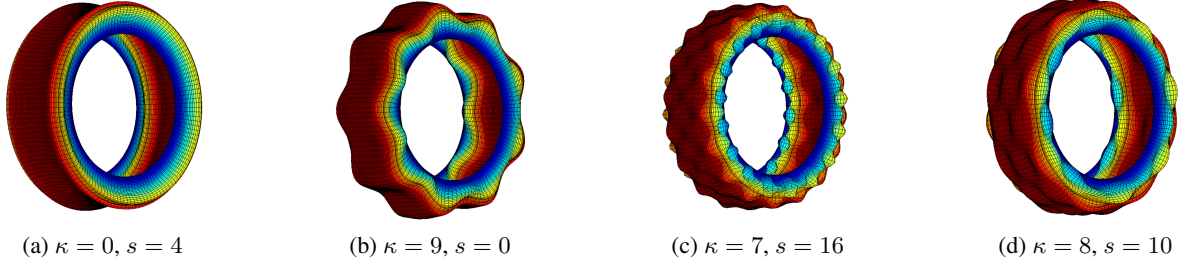


Figure 2 – Examples for free response solutions of type $\Psi_{\kappa,s} e^{-j\kappa\theta}$, where s denotes the cross-sectional mode order. Note that due to the wave ansatz, these deformation shapes are not stationary in circumferential direction but move around the tire. Exceptions are solutions for $\kappa = 0$.

the components of the displacement vector $\mathbf{u} = [u_r \ u_x \ u_\theta]^T$ at a point (r, x, θ) are accordingly given by

$$u_i(r, x, \theta, t) = \mathbf{N}(r, x) \mathbf{v}_i(\theta, t) \quad i = r, x, \theta. \quad (1)$$

Herein, \mathbf{N} is a vector of cross-sectional FE shape functions while \mathbf{v}_i represents the corresponding nodal degrees of freedom vector. Thus, only the displacements' dependence on the cross-sectional coordinates is approximated using FE modeling. The nodal displacements are functions of the angular coordinate θ and depend on the assumed wave propagation along this dimension.

By assuming viscoelastic material properties, harmonic motion of type $e^{j\omega t}$ (where t is the time, ω the angular frequency and $j = \sqrt{-1}$), and the absence of volume forces and external traction, variational principles and standard procedures for finite element formulation can be used to obtain a set of coupled ordinary differential equations [22]:

$$\left[-\mathbf{A}_{11} \frac{\partial^2}{\partial \theta^2} + (\mathbf{A}_{01} - \mathbf{A}_{10}) \frac{\partial}{\partial \theta} + \mathbf{A}_{00} - \omega^2 \mathbf{M} \right] \mathbf{v}(\theta, \omega) = \mathbf{f}(\theta, \omega). \quad (2)$$

The generalized stiffness matrices \mathbf{A}_{nm} and the mass matrix \mathbf{M} are derived from the tire's potential respectively kinetic energies and \mathbf{f} is the generalized force vector describing the external load. By setting $\mathbf{f} = 0$, the homogeneous case is obtained for which solutions are given by exponential functions of type

$$\mathbf{v}(\theta, \omega) = \Psi(\omega) e^{-j\kappa\theta}. \quad (3)$$

These functions can be physically interpreted as waves of cross-sectional mode shape Ψ propagating along the circumferential direction with polar wave number κ . Inserting (3) into (2) results in an eigenvalue problem which can be solved to get the eigenfrequencies and cross-sectional mode shapes⁵ for a specific polar wave number κ . Some examples for different $\Psi_{\kappa,s}$, where s is the cross-sectional mode order, are shown in Figure 2. The solution to the inhomogeneous form of (3), i.e. the forced response case $\mathbf{f} \neq 0$, is obtained using a modal summation procedure as described in [22, 23].

In the cross-section modeling (cf. Figure 1b), 12 isotropic, two-dimensional solid elements of Lagrange type with nine nodes are used for the tread. The sidewalls and the belt consist of 37 anisotropic, doubly-curved deep shell elements accounting for rotational inertia, shearing across the thickness, and pretension due to tire inflation. The shape functions are quadratic. Detailed derivations of both element types are given in [18].

The quasi-static simulations in this study are performed using a non-linear 3D tire/road interaction method which is usually used to simulate the interaction between a rolling tire and a real (non-smooth) road surface [22]. The contact problem formulation reads

⁵ There is always some confusion in the use of the terms *modes* and *waves* in connection with tires. Due to the wave ansatz and the high structural damping, it is appropriate to speak of *waves* in circumferential direction. The solutions for the cross-sectional motion are obtained as the eigenvectors for a particular κ , which is similar to how mode shapes are obtained for simpler structures. Hence, the cross-sectional motion will be referred to as *modes*.

$$\mathbf{u}(t_N) = \mathbf{G}_0 \mathbf{F}(t_N) + \mathbf{u}_{\text{old}}(t_N) \quad (4a)$$

$$F_e(t_N) = k d_e(t_N) \mathcal{H}(d_e(t_N)) \quad (4b)$$

$$\mathbf{d}(t_N) = \mathbf{Z}_R(t_N) - \mathbf{Z}_T(t_N) - \mathbf{u}(t_N). \quad (4c)$$

\mathbf{u} and \mathbf{F} denote the normal tire displacements and contact forces at time step t_N . \mathbf{G}_0 contains the values of the tire's Green's function for $t_N = 0$. \mathbf{u}_{old} is the displacement given by the contribution from previous time steps, and \mathbf{Z}_R and \mathbf{Z}_T are the road roughness and tire profiles. \mathcal{H} is the Heaviside function and the subscript e denotes one individual contact point. To account for small-scale roughness phenomena and the resulting difference between the apparent and real area of contact, contact springs are introduced between the tire and the road. This is reflected by the spring stiffness k in (4b). For the quasi-static simulations contact is calculated for a non-rotating tire on a smooth surface.

4 INPUT DATA

The considered tire is of type 175/65R 14T XL. In both models only the tire structure is modeled, while the effect of the inflation pressure of 200 kPa is captured either by a pressure (FEM) or a pretension (WFEM) mechanisms. The air cavity is not explicitly modeled as the fluid/structure coupling is of minor relevance for tire vibrations [15] unless hub forces are considered. The wheel is also not included in the model. Tyre motion is blocked at the bead.

The tire geometry (including the material sections) and bulk material properties are known and shared between both models. Due to the simplified nature of the cross-sectional mesh used in the WFE simulations, a condensation procedure is necessary to derive the corresponding material properties of the shell elements constituting of several different material groups. The procedure is based on classical lamination theory. Details about the condensation procedure and further property optimization with respect to measured radial mobilities can be found in [22]. In the FE model, the different material groups are modeled individually and no further material optimization is performed. In both tire models viscoelastic properties for 20 °C and 200 Hz are used. The WFE model's original purpose is to simulate tire vibrations due to tire/road interaction, meaning that both contact deformation and dynamic response are determined simultaneously. Accordingly, in this study viscoelastic properties are used for both the quasi-static and the dynamic WFE simulations. In the case of FEM, the standard procedure of considering viscoelasticity only for the dynamic simulations is followed. A common proportional damping model using an eigenfrequency depending loss-factor is incorporated in both models.

5 SIMULATION RESULTS

5.1 Quasi-static simulations

In Figure 3 the predicted tire footprint sizes for both methods are compared to each other for five different tire loads. For a load of 3000 N both methods give approximately the same footprint size. For lower loads, WFEM overestimates the footprint area in comparison to the FEM results, with a maximum area deviation of 44 % for 1000 N. In contrast, for higher loads WFEM underestimates the area, at most with 24 % at 5000 N. All variations in area are mostly due to differences in the circumferential direction;

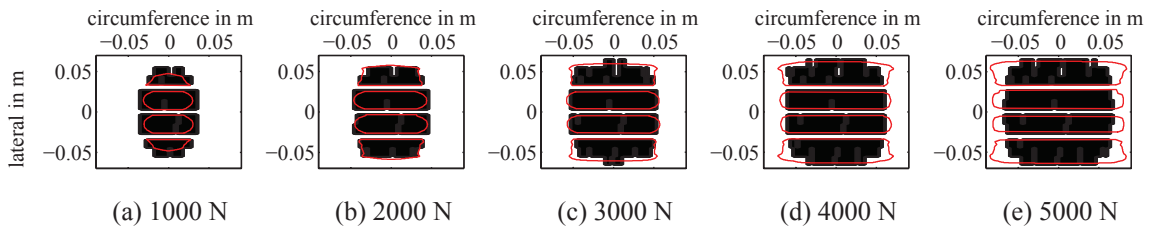


Figure 3 – Size of footprint area for different tire loads for FE (—) and WFE simulations (solid black area).

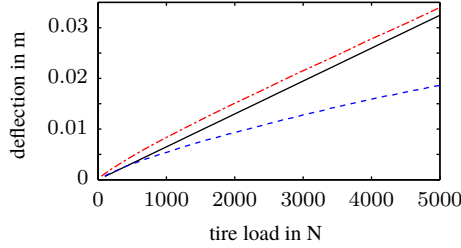


Figure 4 – Load-deflection curves for FE (---) and WFE simulations (---) and Equation (5) (—).

the footprint size in lateral direction matches well between both methods apart from the case of 1000 N load.

Considerably bigger differences between FE and WFE simulations are visible in the load-deflection curves plotted in Figure 4. While both curves exhibit the expected slight non-linearity [24], for any given load the deflection in the FE model is always considerably higher than that in the WFE model. The differences between the two models rise from 56 % at 1000 N to 82 % at 5000 N. Also plotted in Figure 4 is an empirical linear load-deflection approximation (see [24]) given as

$$d = L \cdot (0.00028P \sqrt{(-0.004AR + 1.03)S_N(S_N AR/50 + D_R)} + 3.45)^{-1}, \quad (5)$$

where d is the deflection, L the load in kg, P the inflation pressure in kPa, AR and S_N are the aspect ratio and nominal section width as printed on the tire, and D_R is the rim diameter in mm. The FE results are roughly of the same order as these approximation results.

5.2 Dynamic simulations

In Table 1 results of FE and WFE eigenfrequency analyses are compared to measured eigenfrequencies. With the sole exception of the last eigenmode, the FE predictions are always within 10 % of the measured frequencies. The highest differences generally occur for asymmetric mode shapes. The average deviation over all modes is 4.2 %. The WFEM simulations exhibit considerable variations of more than 20 % from the measured eigenfrequencies for the telescopic and rocking semi-rigid modes and the asymmetric mode of circumferential order two. For the rotational semi-rigid mode and the mode of circumferential order nine, deviations are more than 10 %. All other eigenfrequencies are predicted with less than 10 % error, with an average of 9.5 %. Contrary to the FE results, there is no clear difference in accuracy between predictions of symmetric and asymmetric modes.

For the sake of brevity mode shapes predictions cannot be shown here. Agreement between FE and

Table 1 – Measured and simulated eigenfrequencies. SR: semi-rigid, S: symmetric, AS: asymmetric.

circumferential order	mode shape	measured, Hz	FEM, Hz	WFEM, Hz
0	SR: telescopic	40	41	55
0	SR: rotational	63	61	72
1	SR: rocking	50	52	68
1	SR: translational	82	82	86
2	S/AS	106/96	106/94	108/115
3	S/AS	131/157	129/143	134/167
4	S/AS	157/196	153/178	164/204
5	S/AS	184/217	179/204	196/234
6	S/AS	212/244	205/227	228/262
7	S/AS	241/265	233/250	259/290
8	S/AS	270/295	262/273	291/317
9	S	367	291	322

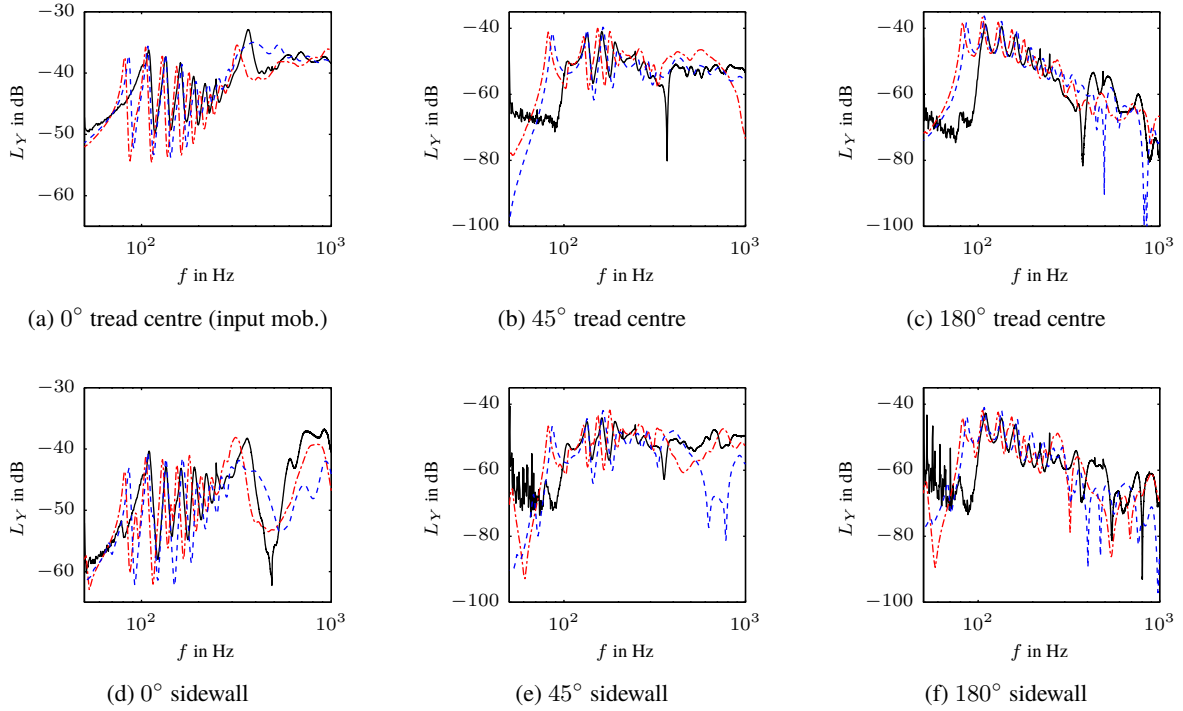


Figure 5 – Comparison of mobilities from measurement (—), WFEM (---), and FE simulations (— · —), with $L_Y = 20 \log_{10}(|Y/Y_0|)$, $Y_0 = 1 \text{ N}/(\text{ms})$, and Y being the mobility.

WFEM simulations is generally good. Minor deviations in mode shape are only visible for higher order modes in the shoulder and sidewall sections. However, due to the fundamental differences in the respective cross-section meshes a more thorough assessment is difficult.

Measured and simulated mobilities for three circumferential angles and positions on the tire sidewall and near the tread centre line are given in Figure 5. In the measurements the rim is not fixed as in the simulations, but freely suspended. Due to this all simulated mobilities have an additional low frequency resonance which is not visible in the measurements. This peak is caused by the translational semi-rigid body mode. Starting with the input mobility in Figure 5a, it can be observed that the WFEM results match better with the measured mobility in the frequency range from 100 Hz to roughly 260 Hz than the FEM simulations do. Between 260 Hz and 500 Hz neither simulation result is particularly good. In contrast to the WFEM results, FE results at least exhibit a similar shape compared to the measurements. Above 500 Hz WFEM again seems to be slightly closer to the measured mobility amplitudes than FEM is. Noteworthy is also that the amplitudes of the first four (WFEM) respectively seven (FEM) simulated anti-resonances are considerably lower than the measured ones.

Figures 5b and 5c show transfer mobilities to positions on the tread centre line at circumferential angles of 45° and 180° to the excitation. Similar tendencies as for the input mobility are visible with WFEM performing better than FEM in low frequency regions up to 200 Hz (45°) and 260 Hz (180°), and high-frequency regions above 500 Hz. For intermediate frequencies both methods show some deviations from the measured mobility. Yet, general tendencies are still captured equally well by both methods.

In Figures 5d and 5e the transfer mobilities for a position at the tire sidewall and circumferential angles of 0° and 45° are shown. Though the first two measured resonances are better approximated by WFEM, both methods are having equal difficulties to correctly determine resonance frequencies and amplitudes up to 300 Hz. Yet, for frequencies between 120 Hz and 450 Hz the WFEM prediction is closer to the measured mobility than the FEM result. For higher frequencies only FEM is capable of capturing the general features and amplitude levels of the measured mobility. Finally, for a sidewall position at 180° (Figure 5f) WFEM is again better for lower frequencies up to 180 Hz. For higher frequencies both methods

struggle somewhat to accurately predict the measured mobility in detail. FEM, though, is remarkably precise in the prediction of the resonances at 347 Hz and 890 Hz, and the anti-resonance at 546 Hz.

6 DISCUSSION

Looking at the quasi-static simulations, three major observations can be made: Firstly, the WFE footprint predictions are remarkably good for a dynamic model which is not optimized for static calculations. Secondly, and this is linked to the previous observation, the influence of the contact spring stiffness k in Equation (4) has to be taken into account in the footprint analysis. The stiffness is load-dependent; yet, in this study a constant value derived for a load of 2820 N is used. This partly explains the good match for the load of 3000 N and the over- and underestimations for lower respectively higher loads. Thirdly, in contrast to the footprint analysis, there are major differences in the load-deflection analysis between the WFE results on the one hand and the FE and empirical approximation results on the other hand. This is seen as an indication that the stiffness of the tire's sidewall in the WFE model is too high. Indeed, the FE model can capture the non-linear softening of the sidewall membrane under loading. This is not possible in WFEM as the sidewall is modeled according to its inflated geometry. Additionally, there might be problems with modeling the entire sidewall thickness by one layer of shell elements; e.g. in terms of material parameter estimation or element stiffness.

An important observation for the dynamic analysis is the fact that the measurement results for the eigenfrequency analysis and the mobility measurements show some discrepancies, as can be expected for a viscoelastic structure. Free and forced response measurements correspond to different strain conditions for the rubber components of the tire, resulting in different dynamic stiffness properties. The extent of the observed discrepancies depends on the participation of the rubber stiffness in each of the modes.

The telescopic, rotational, and rocking semi-rigid body modes are not visible in the measured mobilities. Hence, they are not accounted for in the WFE material optimization process. The fact that all of these modes are mainly dependent on sidewall stiffness (and partly pretension) supports the previously made assumption that the sidewall stiffness of the WFE model is too high. A possible incorrect sidewall modeling in WFE is also indicated in the mobility plots in Figure 5. This may be taken as an indication of the complexity of the model property update process, given that the influence of complete construction zones can be dominant in one test and completely absent in another.

In view of an optimization of material properties with regards to mobilities ranging up to 1 kHz, it is also rather unfortunate to use 200 Hz as reference frequency for the viscoelastic properties. For large parts of the frequency range initial material values are too soft; yet this was a conscious choice given the requirement to include contact deformation calculation in WFEM. By accounting for this in the optimization process, the WFE tire model becomes overly stiff for frequencies considerably lower than 200 Hz. This is visible in the semi-rigid body modes and the quasi-static calculations (which are basically the extreme $f = 0$ case of the dynamic simulations). Although the FE model is also based on material values for 200 Hz, it does not exhibit the same problems as the WFE model. This can be partly explained by the fact that no further adjustment of material parameters is done which could lead to a stiffening of the model. The effect of this can be seen in the high-frequency regions of the mobilities on the tread centre line which are slightly worse than those predicted by WFEM.

It shall be emphasized that predicting dynamic properties by an eigenanalysis method has some inherent difficulties. The stiffness property of the viscoelastic parts of the tire is extremely sensitive to temperature, frequency and strain conditions. Although specific constant values of these properties may be *a priori* chosen, this will always be some sort of compromise for the various zones of the tire, depending on the nature of the excitation. It may be argued that the good free response accuracy performance (hammer excitation) shown by the FE model and the worse forced response one (shaker excitation) shows exactly the effect of these compromises. Obviously, the material parameter updating for the WFE model largely compensates for this effect, but this does not come without a negative impact on its correlation to the free response test results. Another difference between the models is that the geometry and the different material groups are included in detail in the FE model, whereas geometric simplifications and material condensation are used in the WFE model.

7 FINAL REMARKS

The performance of a waveguide finite element model — optimized for radial mobility test performance — and a finite element model of car tire are compared with regards to quasi-static and dynamic simulations. There is good agreement in footprint sizes prediction; differences for particularly low or high tire loads can be explained by the influence of the contact spring stiffness parameter in the WFE model and the linear nature of the tire model. This is a significant result since the typical WFEM application case is the simulation of tire vibrations induced by rolling tire/road interaction. This not only requires proper modeling of the dynamic tire response but also of contact area in which the road excitation acts. Large differences in the modeling of the load-deflection curves indicate problems in the sidewall representation in the WFE model. This assumption is supported by the results of the eigenfrequency study, where WFEM considerably overestimates the eigenfrequencies for the lowest modes. Predictions of higher order eigenfrequencies and mobilities are reasonably accurate in both models. Parts of the differences between the models can be explained by the one-sided optimization of the WFE model towards mobility simulations, where not all sidewall effects are visible. It can be expected that the differences between the models are smaller when additional information such as eigenfrequency measurements are taken into account for the WFE material optimization. With regard to viscoelasticity effects, the strain differences between free and forced response excitation and the varying frequency conditions have an impact on the accuracy of both models. In WFEM this is partly compensated by the material updating. In summary, the presented WFE tire model generally seems to be capable of producing results of the same quality as the FE tire model does. However, it seems that the WFE model needs more optimizing for the particular task than FEM, where the same basic model gives good results for quasi-static and dynamic simulations only depending on whether viscoelasticity is included or not.

Finally, a few comments on utilization differences between the two methods shall be added. The big advantage of using an FE model with detailed modeling of material groups is the flexibility to handle material data and model changes. In the current WFE model, in contrast, a somewhat complex condensation of material properties is necessary due to the wide use of shell elements. In fact, this becomes an advantage if the possibility of using an update method for the improvement of the correlation to a particular kind of test (such as the radial mobility here) is considered. The complexity of the FE representation does not allow for the robust application of similar methods and the correlation depends largely on the quality and the properties of the initial model set up.

An advantage of WFEM is that post-processing considerably easy because of the inherent differentiation between cross-sectional modes shapes and circumferential waves, which facilitates easy data analysis. WFEM is also numerically much more efficient; though practically no difference in the mobility calculation workload exists (given that both models use a modal representation at this level), the preceding modal expansion step takes significantly larger time for the FE model. This makes WFEM well suited for parameter studies where not the full capabilities of FEM are needed. This emphasizes that WFEM is not competing with FEM; it is rather complementing it.

ACKNOWLEDGEMENTS

The funding from the BMWi project *LeiStra3* (Leiser Straßenverkehr 3) is gratefully acknowledged.

References

- [1] Regulation (EC) No 1222/2009. EC Official Journal L, 342, 46–58 (2009).
- [2] Regulation (EC) No 661/2009. EC Official Journal L, 200, 1–24 (2009).
- [3] W. van Keulen and M. Duškov, “Inventory study of basic knowledge on tyre/road noise”, Report DWW-2005-022, IPG (2005).
- [4] W. Kropp, F.-X. Becot and S. Barrelet, “On the sound radiation from tyres”, *Acta Acust. United Ac.*, 86, 769–779 (2000).
- [5] F. Böhm, “Mechanik des Gürtelreifens”, *Arch. Appl. Mech.*, 35, 82–101 (1966).

- [6] L. Kung, W. Soedel and T. Yang, “Free vibration of a pneumatic tire-wheel unit using a ring on an elastic foundation”, *J. Sound Vib.*, 107(2), 181–194 (1986).
- [7] P. Kindt, P. Sas and W. Desmet, “Development and validation of a three-dimensional ring-based structural tyre model”, *J. Sound Vib.*, 326(3–5), 852–869 (2009).
- [8] A. Tsotras, *On the interaction between modal behaviour and contact force development of a pneumatic tyre* (PhD thesis, Loughborough University, 2010).
- [9] W. Kropp, “Structure-borne sound on a smooth tyre”, *Appl. Acoust.*, 26(3), 181–192 (1989).
- [10] J. Muggleton, B. Mace and M. Brennan, “Vibrational response prediction of a pneumatic tyre using an orthotropic two-plate wave model”, *J. Sound Vib.*, 264(4), 929–950 (2003).
- [11] K. Larsson and W. Kropp, “A high-frequency three-dimensional tyre model based on two coupled elastic layers”, *J. Sound Vib.*, 253(4), 889–908 (2002).
- [12] R. Pinnington, “A wave model of a circular tyre” (Parts 1 and 2), *J. Sound Vib.*, 290(1–2), 101–168 (2006).
- [13] C. Lecomte, W. Graham and M. Dale, “A shell model for tyre belt vibrations”, *J. Sound Vib.*, 329(10), 1717–1742 (2010).
- [14] S. Saigal, T. Yang, H. Kim, and W. Soedel, “Free vibrations of a tire as a toroidal membrane”, *J. Sound Vib.*, 107(1), 71–82 (1986).
- [15] T. Richards, “Finite element analysis of structural-acoustic coupling in tyres”, *J. Sound Vib.*, 149(2), 235–243 (1991).
- [16] M. Brinkmeier, U. Nackenhorst, S. Petersen and O. von Estorff, “A finite element approach for the simulation of tire rolling noise”, *J. Sound Vib.*, 309(1–2), 20–39 (2008).
- [17] I. Lopez, R. Blom, N. Roozen and H. Nijmeijer, “Modelling vibrations on deformed rolling tyres – a modal approach”, *J. Sound Vib.*, 307(3–5), 481–494 (2007).
- [18] S. Finnveden and M. Fraggstedt, “Waveguide finite elements for curved structures”, *J. Sound Vib.*, 312(4–5), 644–671 (2008).
- [19] P. Sabiniarz and W. Kropp, “A waveguide finite element aided analysis of the wave field on a stationary tyre, not in contact with the ground”, *J. Sound Vib.*, 329(15), 3041–3064 (2010).
- [20] Y. Waki, B. Mace and M. Brennan, “Free and forced vibrations of a tyre using a wave/finite element approach”, *J. Sound Vib.*, 323(3–5), 737–756 (2009).
- [21] Y. Waki, B. Mace and M. Brennan, “Numerical issues concerning the wave and finite element method for free and forced vibrations of waveguides”, *J. Sound Vib.*, 327(1–2), 92–108 (2009).
- [22] C. Hoever, *The influence of modeling parameters on the simulation of car tyre rolling losses and rolling noise* (Licentiate thesis, Chalmers University of Technology, Gothenburg, 2012). Available at: <http://publications.lib.chalmers.se/records/fulltext/166543/166543.pdf>
- [23] W. Kropp, P. Sabiniarz, H. Brick and T. Beckenbauer, “On the sound radiation of a rolling tyre”, *J. Sound Vib.*, 331(8), 1789–1805 (2012).
- [24] A. Gent and J. Walter (Eds.), *The pneumatic tire* (U.S. Department of Transportation, National Highway Safety Administration, 2006).